Layered Tin(II) Oxalates Possessing Large Apertures

Srinivasan Natarajan,[†] R. Vaidhyanathan,[†] C. N. R. Rao,*[,†] S. Ayyappan,[‡] and Anthony K. Cheetham*[,‡]

Chemistry and Physics of Materials Unit, Jawaharlal Nehru Centre for Advanced Scientific Research, Jakkur Campus, Jakkur P.O., Balgalore 560 064, India, and Materials Research Laboratory, University of California, Santa Barbara, California 93106

Received March 1, 1999. Revised Manuscript Received April 12, 1999

Two layered tin(II) oxalate structures have been prepared by hydrothermal methods in the presence of structure-directing organic amines. The crystal data for these structures are as follows: oxalate **I**, $[(CH_3)_2NH(CH_2)_2NH(CH_3)_2]^{2+}[Sn_2(C_2O_4)_3]^{2-}\cdot H_2O$, monoclinic, space group *C*2/*c* (no. 15), $a = 16.567$ (8) Å, $b = 10.851$ (6) Å, $c = 11.652$ (6) Å, $\beta = 102.62$ (3)°, $V = 2039.0$ (1) Å^3, $Z = 4$, $M = 637.4(1)$, $D_{calc} = 2.825$ g cm^{-3}, Mo Kα, $R_F = 0.04$; oxalate **II**, $[C(NH_2)_3]_2^{+}[Sn_4(C_2O_4)_5]^{2-}\cdot 2H_2O$, orthorhombic, space group *Pbca* (no. 61), $a = 11.390$ (1) Å, $b = 14.742$ (1) Å, $c = 16.755$ (1) Å, $V = 2813.1$ (1) Å^3, $Z = 8$, $M = 1070.8(1)$, $D_{calc} = 2.844$ g cm^{-3}, Mo Kα, $R_F = 0.06$. In **I**, pseudo-pentagonal-bipyramidal SnO_6 units form a puckered layered structure by sharing oxygens with the oxalate anions. The layers contain 8- and 12-membered apertures, and the amine (protonated *N*,*N*,*N*′*N*′-tetramethyl-1,2-diaminoethane) and water molecules are in the interlamellar region where they interact with the framework and with each other by hydrogen bonding. The lone pairs of the Sn(II) atoms point into the interlamellar region. Oxalate **II** contains both square-pyramidal SnO_4 units and SnO_6 units similar to those in **I**. These units together form a saw-tooth lamellar structure by linking through the oxalates. The sheets contain 20-membered corrugated rings, which hold two amine cations (guanidinium) and two water molecules, which interact with the framework via hydrogen bonding.

Introduction

The synthesis of novel open-framework structures has emerged as an important area of research because of their potential use in separation processes and catalysis.[1] Synthesis of these materials generally makes use of structure-directing agents (SDAs), as is common in the preparation of zeolitic materials.[2] A large number of open-framework solids based on metal phosphates has been synthesized and characterized in the past decade.[2] Metal phosphonates and diphosphonates possessing open structures have been synthesized and characterized by Haushalter et al.[3−5] and others,[6−8] and the synthesis of framework solids based on chalcogenides, pnictides, cyanides, and thiopnictates has also been accomplished.[9] Interestingly, organic porous solids mimicking the behavior of inorganic porous solids have been synthesized only in the last two or three years.[10−12] Rigid bidentate ligands linked with metal centers are known to form open networks,[13] and carboxylates of metals with new open architectures, possessing interesting physical properties (e.g., reversible hydration/dehydration), have been reported in the last three to four years.[14−18] A new family of tin oxalates containing SDAs was reported a few months ago, including two monomers having 4-coordinated Sn(II) and one sheet structure having 6-coordinated Sn(II).[19] On the basis of our experience with open-framework tin phosphates,[20−24]

* Corresponding authors.
[†] Jawaharlal Nehru Centre for Advanced Scientific Research.
[‡] University of California.

(1) Cheetham, A. K.; Férey, G.; Loiseau, T. *Angew. Chem.* **1999**, in press.
(2) Meier, W. M.; Olson, D. H. *Atlas of Zeolite Structure Types*; Butterworths: London, 1992.
(3) Bowes, C. L.; Ozin, G. A. *Adv. Mater.* **1996**, *8*, 13 and references therein.
(4) LaDuca, R.; Rose, D.; Debord, R. J. D.; Haushalter, R. C.; O'Connor, C. J.; Zubieta, J. *J. Solid State Chem.* **1996**, *123*, 408.
(5) Bonavia, G. H.; Haushalter, R. C.; Lu, S.; O'Connor, C. J.; Zubieta, J. *J. Solid State Chem.* **1997**, *132*, 144.
(6) Zapf, P. J.; Rose, D. J.; Haushalter, R. C.; Zubieta, J. *J. Solid State Chem.* **1996**, *125*, 192; *J. Solid State Chem.* **1997**, *132*, 438.
(7) Clearfield, A. *Chem. Mater.* **1998**, *10*, 2801 and references therein. Poojary, D. M.; Hu, H.-L.; Campbell, F. L., III.; Clearfield, A. *Acta Crystallogr.* **1993**, *B49*, 996.
(8) Riou, D.; Férey, G., *J. Mater. Chem.* **1998**, *8*, 2733. Zhang, B.; Poojary, D. M.; Clearfield, A. *Inorg. Chem.* **1998**, *37*, 1844.
(9) Bowes, C. L.; Ozin, G. A. *Adv. Mater.* **1996**, *8*, 13. Conrad, O.; Jansen, C.; Krebs, B. *Angew. Chem., Int. Ed.* **1998**, *37*, 3208.
(10) Losier, P.; Zaworotko, M. J. *Angew. Chem., Int. Ed. Engl.* **1996**, *35*. 2779. Zaworotko, M. J. *Chem. Soc. Rev.* **1994**, 283.
(11) Yaghi, O. M.; Li, H. *Angew. Chem., Int. Ed. Engl.* **1995**, *34*, 207. Yaghi, O. M.; Li, H. *J. Am. Chem. Soc.* **1995**, *117*, 10401. Yaghi, O. M.; Li, H. *Nature* **1995**, *378*, 703.
(12) Pedireddi, V. R.; Chatterjee, S.; Ranganathan, A.; Rao, C. N. R. *J. Am. Chem. Soc.* **1997**, *119*, 10867.
(13) Hagrman, D.; Warren, C. J.; Haushalter, R. C.; Seip, C.; O'Connor, C. J.; Rarig, R. S., Jr.; Johnson, K. M., III; LaBuca, R. L., Jr.; Zubieta, J. *Chem. Mater.* **1998**, *10*, 3294.
(14) Serpaggi, F.; Férey, G. *J. Mater. Chem.* **1998**, *8*, 2737. Livage, C.; Egger, C.; Nogues, C.; Férey, G. *J. Mater. Chem.* **1998**, *8*, 2743.
(15) Romero, S.; Mosset, A.; Trombe, J. C. *Eur. J. Solid State Inorg. Chem.* **1997**, *34*, 209.
(16) Clemente-Leon, M.; Coronado, E.; Galan-Mascaros, J.-R.; Comez-Garcia, C. J. *Chem. Commun.* **1997**, 1727.
(17) Farrell, S. P.; Hambley, T. W.; Lay, P. A. *Inorg. Chem.* **1995**, *34*, 757.
(18) Kitagawa, S.; Okubo, T.; Kawata, S.; Kondo, M.; Katada, M.; Kobayashi, H. *Inorg. Chem.* **1995**, *34*, 4790.
(19) Ayyappan, S.; Cheetham, A. K.; Natarajan, S.; Rao, C. N. R. *Chem. Mater.* **1998**, *10*, 3746.

10.1021/cm990124e CCC: $18.00
Published on Web 05/21/1999

it appeared to us that the tin oxalates may well form a wide variety of open-framework solids with different aperture sizes as well as interesting structural features. We have therefore attempted to synthesize further tin oxalates in the presence of structure-directing amines by hydrothermal methods. Our experiments have yielded a layered material containing 8- and 12- membered rings with *N*,*N*,*N*′,*N*′-tetramethylethylenediamine as the SDA. More importantly, we have been able to obtain another layered material with very large aperture, involving 20-membered rings, by employing guanidine as the SDA.

Experimental Section

Synthesis and Initial Characterization. The tin(II) oxalates, **I** and **II**, were synthesized starting from a mixture containing *N*,*N*,*N*′,*N*′-tetramethylethylenediamine (TMED) and guanidinium carbonate (GC), respectively, as the SDAs. For **I**, tin(II) oxalate, phosphoric acid (85 wt %), TMED and water in the ratio SnC_2O_4:H_3PO_4:TMED:$55H_2O$ were taken in the starting mixture. For **II**, tin oxalate, phosphoric acid, GC, and water were mixed in the ratio SnC_2O_4:$2H_3PO_4$:GC:$55H_2O$ (all the chemicals used in the synthesis were obtained from Aldrich). The starting mixtures were stirred to attain homogeneity, transferred into a 23-mL (fill factor = 40%) PTFE bottle, and sealed in a stainless steel autoclave (Parr, Moline, IL). The sealed pressure bombs were heated at 150 °C for 48 h for **I** and 36 h for **II** under autogenous pressure. The resulting products, which contained a small quantity of crystals along with white powder, were filtered and washed thoroughly with deionized water. The single crystals were easily separated from the white powder under an optical microscope. Powder X-ray diffraction (XRD) patterns on the powdered crystals indicated that the products were new; the pattern is entirely consistent with the structure determined by single-crystal X-ray diffraction. In the case of **I**, the white powder as well as the crystals were identical as determined by powder XRD. In the case of **II**, however, the powder was a condensed tin phosphate, but the crystals were of the open framework tin oxalate phase. The as-prepared powder sample of **II** was found to contain some impurities which we have not identified. Thermogravimetric analysis (TGA) was carried out in static air in the range between 25 and 900 °C.

Single-Crystal Structure Determination. A suitable single crystal of each compound was carefully selected under a polarizing microscope and glued to a thin glass fiber with cyanoacrylate (super glue) adhesive. Single-crystal structure determination by X-ray diffraction was performed on a Siemens Smart-CCD diffractometer equipped with a normal focus, 2.4 kW sealed tube X-ray source (Mo Kα radiation, λ = 0.710 73 Å) operating at 50 kV and 40 mA. A hemisphere of intensity data was collected at room temperature in 1321 frames with ω scans (width of 0.30° and exposure time of 20 s per frame) in the 2θ range 3 to 46.5°. Pertinent experimental details for the structure determinations are presented in Table 1.

The structure was solved by direct methods using SHELXS-86[25] and difference Fourier syntheses. All the hydrogen positions for both compounds were initially located in the difference Fourier maps, but for the final refinement the hydrogen atoms were placed geometrically. In the case of **II**, the hydrogen atoms of the amine molecules were placed assuming a planar sp^2 hybridization about each N atom with a N−H bond length of 0.86 Å. Hydrogens were held in the riding mode for both compounds. No absorption corrections were applied. The last cycles of refinement included atomic positions for all the atoms, anisotropic thermal parameters for all non-hydrogen atoms and isotropic thermal parameters for all the hydrogen atoms. Full-matrix least-squares structure refinement against $|F^2|$ was carried out using the SHELXTL-PLUS[26] package of programs. Details of the final refinements are given in Table 1. The final atomic coordinates, and selected bond distances and angles for **I** are presented in Tables 2, 3, and 4, and for **II** in Tables 5, 6, and 7.

Table 1. Crystal Data and Structure Refinement Parameters for I, $[(CH_3)_2NH(CH_2)_2NH(CH_3)_2]^{2+}[Sn_2(C_2O_4)_3]^{2-}\cdot H_2O$ and II, $2[C(NH_2)_3]^{+}[Sn_4(C_2O_4)_5]^{2-}\cdot 2H_2O$

	I	II
empirical formula	$Sn_2O_{13}C_{12}N_2H_{20}$	$Sn_4O_{22}C_{12}N_6H_{16}$
crystal system	monoclinic	orthorhombic
space group	*C*2/*c* (no. 15)	*Pbca* (no. 61)
crystal size (mm)	0.06 × 0.08 × 0.2	0.04 × 0.12 × 0.12
a (Å)	16.567(8)	11.390(1)
b (Å)	10.851(6)	14.742(1)
c (Å)	11.652(6)	16.755(1)
β (deg)	102.62(3)	90.0
V (Å^3)	2038.6(2)	2813.1(1)
Z	4	8
formula mass	637.4(1)	1070.8(1)
ρ_{calc} (g cm^{-3})	2.825	2.844
λ (Mo Kα) Å	0.71073	0.71073
μ (mm^{-1})	5.813	5.851
θ range	2.26−23.29	2.43−25.00
total data collected	4180	20932
index ranges	$-18 \le h \le 15$, $-12 \le k \le 9$, $-12 \le l \le 12$	$-15 \le h \le 15$, $-19 \le k \le 19$, $-21 \le l \le 22$
unique data	1466	2478
observed data ($I > 2\sigma(I)$)	1042	1341
refinement method	full-matrix least-squares on $\|F^2\|$	full-matrix least-squares on $\|F^2\|$
R_{merg}	0.059	0.27
R indexes [$I > 2\sigma(I)$]	$R_1 = 0.043$,[a] $wR_2 = 0.10$[b]	$R_1 = 0.063$, $wR_2 = 0.122$
R (all data)	$R_1 = 0.080$, $wR_2 = 0.13$	$R_1 = 0.140$, $wR_2 = 0.145$
goodness of fit (S_{obs})	1.08	1.11
goodness of fit (S_{all})	1.05	0.942
no. of variables	136	208
largest difference map peak and hole (eÅ^{-3})	0.790 and −1.014	0.952 and −1.647

[a] $R_1 = \sum||F_0| - |F_c||/\sum|F_0|$. [b] $wR_2 = \{\sum[w(F_0^2 - F_c^2)^2]/\sum[w(F_0^2)^2]\}^{1/2}$. $w = 1/[\sigma^2(F_0)^2 + (aP)^2 + bP]$, $P = [\max(F_0^2,0) + 2(F_c)^2]/3$, where $a = 0.0433$ and $b = 0.0$ for **I** and $a = 0.0501$ and $b = 0.0$ for **II**.

Results

Structure of I, $[(CH_3)_2NH(CH_2)_2NH(CH_3)_2]^{2+}[Sn_2(C_2O_4)_3]^{2-}\cdot H_2O$. The asymmetric unit of **I** contains 15 non-hydrogen atoms (Figure 1a) and the structure consists of macroanionic sheets of formula $[Sn(C_2O_4)_{1.5}]^-$ with interlamellar $[(CH_3)_2NH(CH_2)_2NH(CH_3)_2]^{2+}$ ions. The framework is made up of a network of SnO_6 units [with pseudo-pentagonal-bipyramidal geometry (Figure 1b), assuming that one of the vertexes is occupied by the lone-pair of electrons] and C_2O_4 moieties, which are linked to form puckered sheets that are stacked along *a* (Figures 2−4). The lone pairs of electrons on Sn(II)

(20) Natarajan, S.; Cheetham, A. K. *Angew. Chem., Int. Ed. Engl.* **1997**, *36*, 978.
(21) Natarajan, S.; Ayyappan, S.; Cheetham, A. K.; Rao, C. N. R. *Chem. Mater.* **1998**, *10*, 1627.
(22) Natarajan, S.; Cheetham, A. K. *Chem. Commun.* **1997**, 1089; *J. Solid State Chem.* **1997**, *134*, 207; *J. Solid State Chem.* **1998**, *140*, 435.
(23) Ayyappan, S.; Bu, X.; Cheetham, A. K.; Natarajan, S.; Rao, C. N. R. *Chem. Commun.* **1998**, 2182
(24) Ayyappan, S.; Bu, X.; Rao, C. N. R.; Cheetham, A. K. *Chem. Mater.* **1998**, *10*, 3308.
(25) Sheldrick, G. M. *SHELXL-86 A program for the solution of crystal structures*; University of Göttingen: Göttingen, Germany, 1993.
(26) Sheldrick, G. M. *SHELXS-93 Program for Crystal Structure solution and refinement*, University of Göttingen 1993.

Table 2. Atomic Coordinates (×10⁴) and Equivalent Isotropic Displacement Parameters (Å², ×10³) for I, $[(CH_3)_2NH(CH_2)_2NH(CH_3)_2]^{2+}[Sn_2(C_2O_4)_3]^{2-}\cdot H_2O$

atom	x	y	z	*U*(eq)[a]
Sn(1)	5941(1)	−6076(1)	−15(1)	33(1)
O(1)	6205(4)	−3441(5)	2910(5)	51(2)
O(2)	6551(3)	−8197(5)	−5(5)	39(1)
O(3)	6224(3)	−4276(5)	1167(5)	35(1)
O(4)	7285(3)	−5947(5)	276(5)	36(1)
O(5)	6187(4)	−6533(5)	2097(5)	45(2)
O(6)	6062(4)	−4273(5)	−1203(5)	42(2)
O(100)	5000	−1337(12)	2500	141(6)
C(10)	6199(5)	−4336(8)	2259(8)	35(2)
C(20)	6139(5)	−5647(8)	2749(8)	34(2)
C(30)	7284(5)	−8133(7)	−79(7)	29(2)
N(1)	3548(5)	−1912(8)	4837(8)	51(2)
C(1)	3345(7)	−1182(9)	3695(9)	74(3)
C(2)	4236(7)	−1327(9)	5714(11)	80(4)
C(3)	2816(5)	−2051(7)	5354(8)	41(2)

[a] *U*(eq) is defined as one-third of the trace of the orthogonalized U_{ij} tensor.

Table 3. Selected Bond Distances in I, $[(CH_3)_2NH(CH_2)_2NH(CH_3)_2]^{2+}[Sn_2(C_2O_4)_3]^{2-}\cdot H_2O$

moiety	distance (Å)	moiety	distance (Å)
Framework			
Sn(1)−O(1)[a]	2.596(6)	Sn(1)−O(2)	2.513(6)
Sn(1)−O(3)	2.375(5)	Sn(1)−O(4)	2.182(5)
Sn(1)−O(5)	2.450(6)	Sn(1)−O(6)	2.427(5)
C(10)−O(1)	1.230(10)	C(10)−O(3)	1.280(10)
C(20)−O(5)	1.237(9)	C(20)[a]−O(6)	1.255(9)
C(30)−O(2)	1.237(8)	C(30)[b]−O(4)	1.277(9)
C(10)−C(20)	1.543(11)	C(30)−C(30)[b]	1.54(2)
Organic Moiety			
C(1)−N(1)	1.518(12)	C(2)−N(1)	1.494(13)
C(3)−N(1)	1.475(10)	C(3)−C(3)[c]	1.53(2)

[a] $x, -y-1, z-{}^1/_2$. [b] $-x+{}^3/_2, -y-{}^3/_2, -z$. [c] $-x+{}^1/_2, -y-{}^1/_2, -z+1$.

Table 4. Selected Bond Angles in I, $[(CH_3)_2NH(CH_2)_2NH(CH_3)_2]^{2+}[Sn_2(C_2O_4)_3]^{2-}\cdot H_2O$

moiety	angle (deg)	moiety	angle (deg)
Framework			
O(1)[a]−Sn(1)−O(2)	70.7(2)	O(1)[a]−Sn(1)−O(3)	130.6(2)
O(1)[a]−Sn(1)−O(4)	77.5(2)	O(1)[a]−Sn(1)−O(5)	149.9(2)
O(1)[a]−Sn(1)−O(6)	65.4(2)	O(2)−Sn(1)−O(3)	136.2(2)
O(2)−Sn(1)−O(4)	70.3(2)	O(2)−Sn(1)−O(5)	80.3(2)
O(2)−Sn(1)−O(6)	131.1(2)	O(3)−Sn(1)−O(4)	78.0(2)
O(3)−Sn(1)−O(5)	67.6(2)	O(3)−Sn(1)−O(6)	68.6(2)
O(4)−Sn(1)−O(5)	85.3(2)	O(4)−Sn(1)−O(6)	80.1(2)
O(5)−Sn(1)−O(6)	135.8(2)	O(1)−C(10)−O(3)	124.9(7)
O(5)−C(20)−O(6)[c]	125.0(8)	O(2)−C(30) −O(4)[b]	124.4(7)
O(1)−C(10)−C(20)	119.5(8)	O(2)−C(30)−C(30)[b]	118.6(10)
O(3)−C(10)−C(20)	115.6(8)	O(4)[b]−C(30)−C(30)[b]	117.0(9)
O(5)−C(20)−C(10)	118.2(8)	O(6)[c]−C(20)−C(10)	116.8(8)
Organic Moiety			
C(1)−N(1)−C(2)	111.4(8)	C(1)−N(1)−C(3)	111.4(8)
C(2)−N(1)−C(3)	109.8(8)	N(1)−C(3)−C(3)[d]	111.9(9)

[a] $x, -y-1, z-{}^1/_2$. [b] $-x+{}^3/_2, -y-{}^3/_2, -z$. [c] $x, -y-1, z+{}^1/_2$. [d] $-x+{}^1/_2, -y-{}^1/_2, -z+1$.

project into the interlamellar spaces as shown in Figure 3, and the structure contains 8- (along the *a* axis) and 12-membered (along the *b* axis) apertures. The SDA (protonated *N*,*N*,*N*′*N*′-tetramethyl-1,2-diaminoethane) resides in the 12-membered pores along with water molecules (Figure 3), and these pores penetrate the entire structure in a direction perpendicular to the sheets, yielding a solid with unidimensional channels (∼4.8 × 9.2 Å; longest atom−atom contact distance not including the van der Waals radii). The various hydrogen bonding interactions between the puckered layers and the guest species are best seen in Figure 4.

Table 5. Atomic Coordinates (×10⁴) and Equivalent Isotropic Displacement Parameters (Å², ×10³) for II, $2[C(NH_2)_3]^+[Sn_4(C_2O_4)_5]^{2-}\cdot H_2O$

atom	x	y	z	*U*(eq)[a]
Sn(1)	6307(1)	1785(1)	6805(1)	43(1)
Sn(2)	9094(1)	−1116(1)	8665(1)	46(1)
O(1)	7566(9)	2696(6)	7419(5)	54(3)
O(2)	7506(8)	2383(6)	5850(5)	47(2)
O(3)	7751(7)	794(6)	6782(5)	42(2)
O(4)	6548(7)	1139(7)	8142(5)	49(2)
O(5)	7608(8)	88(6)	8777(6)	53(2)
O(6)	8866(8)	−164(7)	7459(5)	54(3)
O(7)	9156(8)	3158(6)	5668(5)	53(3)
O(8)	9134(10)	3605(8)	7150(6)	80(4)
O(9)	8918(7)	−828(6)	10077(5)	47(2)
O(10)	9780(7)	−44(6)	11032(5)	43(2)
O(100)	8377(15)	2603(15)	9121(10)	141(9)
N(1)	11541(9)	4655(8)	9637(6)	46(3)
N(2)	10132(9)	3936(8)	8953(6)	51(3)
N(3)	10476(11)	3584(8)	10252(7)	61(4)
C(1)	10708(11)	4052(9)	9611(8)	39(3)
C(11)	8346(13)	2861(8)	6099(9)	42(3)
C(12)	8351(14)	3094(10)	7003(9)	53(4)
C(13)	8040(10)	396(10)	7421(8)	36(3)
C(14)	7316(11)	572(9)	8186(8)	41(3)
C(15)	9624(11)	−270(8)	10311(8)	32(3)

[a] *U*(eq) is defined as one-third of the trace of the orthogonalized U_{ij} tensor.

Table 6. Selected Interatomic Distances in II, $2[C(NH_2)_3]^+[Sn_4(C_2O_4)_5]^{2-}\cdot H_2O$

moiety	distance (Å)	moiety	distance (Å)
Framework			
Sn(1)−O(1)	2.217(9)	Sn(1)−O(2)	2.281(9)
Sn(1)−O(3)	2.199(8)	Sn(1)−O(4)	2.449(9)
Sn(2)−O(5)	2.459(9)	Sn(2)−O(6)	2.473(10)
Sn(2)−O(7)[b]	2.525(9)	Sn(2)−O(8)	2.567(10)
Sn(2)−O(9)	2.412(9)	Sn(2)−O(10)[a]	2.197(8)
C(11)−O(2)	1.260(14)	C(11)−O(7)	1.25(2)
C(12)−O(1)	1.28(2)	C(12)−O(8)	1.24(2)
C(13)−O(3)	1.265(14)	C(13)−O(6)	1.25(2)
C(14)−O(4)	1.21(2)	C(14)−O(5)	1.26(2)
C(15)−O(9)	1.216(14)	C(15)−O(10)	1.266(13)
C(11)−C(12)	1.55(2)	C(13)−C(14)	1.55(2)
C(15)−C(15)[a]	1.57(2)		
Organic Moiety			
C(1)−N(1)	1.30(2)	C(1)−N(2)	1.295(14)
C(1)−N(3)	1.30(2)		

[a] $-x+2, -y, -z+2$. [b] $-x+2, y-{}^1/_2, -z+{}^3/_2$. -z+3/2

The Sn−O distances are in the range 2.182−2.596 Å (av 2.424 Å), with the longer distances being associated with the oxygens that are double-bonded to the carbon atoms. The variations in the distances are reflected in the C−O bonding, too (Table 3). The O−Sn−O and O−C−O bond angles are in the range 65.4−149.9° and 124.4−125.0°, respectively (Table 4).

Structure of II, $2[C(NH_2)_3]^+[Sn_4(C_2O_4)_5]^{2-}\cdot 2H_2O$. The asymmetric unit of **II** contains 22 non-hydrogen atoms, including two crystallographically independent Sn atoms, and is shown in Figure 5a. The structure consists of macroanionic sheets of formula $[Sn_2(C_2O_4)_{2.5}]^-$, and charge compensation is achieved by the incorporation of protonated guanidine molecules. Sn(1) is 4-coordinated (forming a distorted square-pyramidal arrangement) and Sn(2) is 6-coordinated (forming a pentagonal-bipyramidal arrangement). As can be seen from Figure 5b, the square-pyramidal and the pseudo-

Table 7. Selected Bond Angles in II, $2[C(NH_2)_3]^+[Sn_4(C_2O_4)_5]^{2-}\cdot H_2O$

moiety	angle (deg)	moiety	angle (deg)
Framework			
O(1)−Sn(1)−O(2)	72.8(3)	O(1)−Sn(1)−O(3)	85.8(3)
O(2)−Sn(1)−O(3)	78.3(3)	O(1)−Sn(1)−O(4)	74.9(3)
O(2)−Sn(1)−O(4)	136.5(3)	O(3)−Sn(1)−O(4)	71.0(3)
O(5)−Sn(2)−O(6)	65.2(3)	O(5)−Sn(2)−O(7)^b	144.7(3)
O(5)−Sn(2)−O(8)^b	134.6(3)	O(5)−Sn(2)−O(9)	75.0(3)
O(5)−Sn(2)−O(10)^a	79.8(3)	O(6)−Sn(2)−O(7)^b	133.3(3)
O(6)−Sn(2)−O(8)^b	71.7(3)	O(6)−Sn(2)−O(9)	133.8(3)
O(6)−Sn(2)−O(10)^a	78.9(3)	O(7)^b−Sn(2)−O(8)^b	64.9(3)
O(7)^b−Sn(2)−O(9)	72.9(3)	O(7)^b−Sn(2)−O(10)^a	76.5(3)
O(8)^b−Sn(2)−O(9)	132.8(3)	O(8)^b−Sn(2)−O(10)^a	78.7(4)
O(9)−Sn(2)−O(10)^a	71.6(3)	O(2)−C(11)−O(7)	124.3(13)
O(1)−C(12)−O(8)	127.1(14)	O(3)−C(13)−O(6)	123.0(11)
O(4)−C(14)−O(5)	128.8(12)	O(9)−C(15)−O(10)	125.4(11)
O(1)−C(12)−C(11)	115.3(13)	O(2)−C(11)−C(12)	116.8(13)
O(3)−C(13)−C(14)	119.0(13)	O(4)−C(14)−C(13)	116.7(13)
O(5)−C(14)−C(13)	114.4(13)	O(6)−C(13)−C(14)	118.0(12)
O(7)−C(11)−C(12)	119.0(12)	O(8)−C(12)−C(11)	117.6(13)
O(9)−C(15)−C(15)^a	119(2)	O(10)−C(15)−C(15)^a	115(2)
Organic Moiety			
N(1)−C(1)−N(2)	119.2(12)	N(1)−C(1)−N(3)	118.9(12)
N(2)−C(1)−N(3)	122.0(13)		

^{a} $-x+2, -y, -z+2$. ^{b} $-x+2, y-{}^1/_2, -z+{}^3/_2$. -z+3/2.

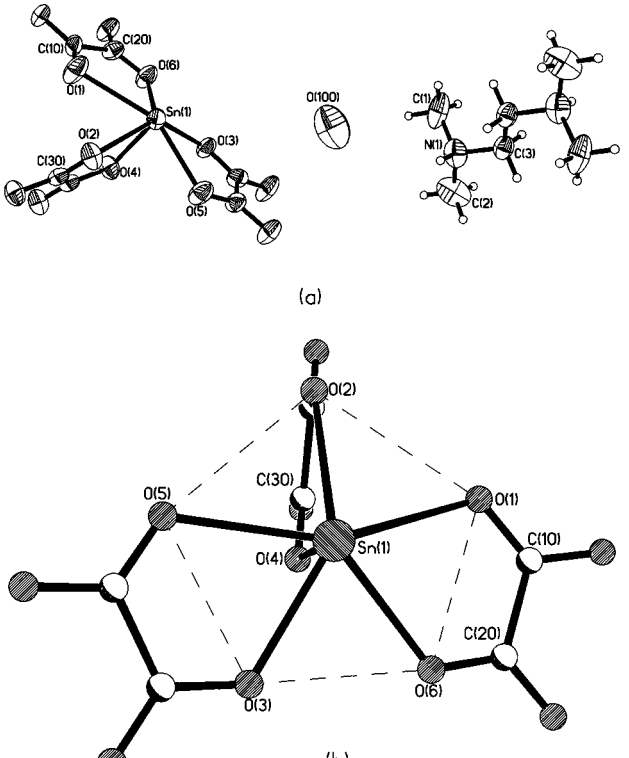

Figure 1. (a) ORTEP plot of **I**, $[(CH_3)_2NH(CH_2)_2NH(CH_3)_2]^{2+}[Sn_2(C_2O_4)_3]^{2-}\cdot H_2O$ showing the connectivity (asymmetric unit is labeled). Thermal ellipsoids are given at 50% probability. (b) View showing the stereochemistry around Sn.

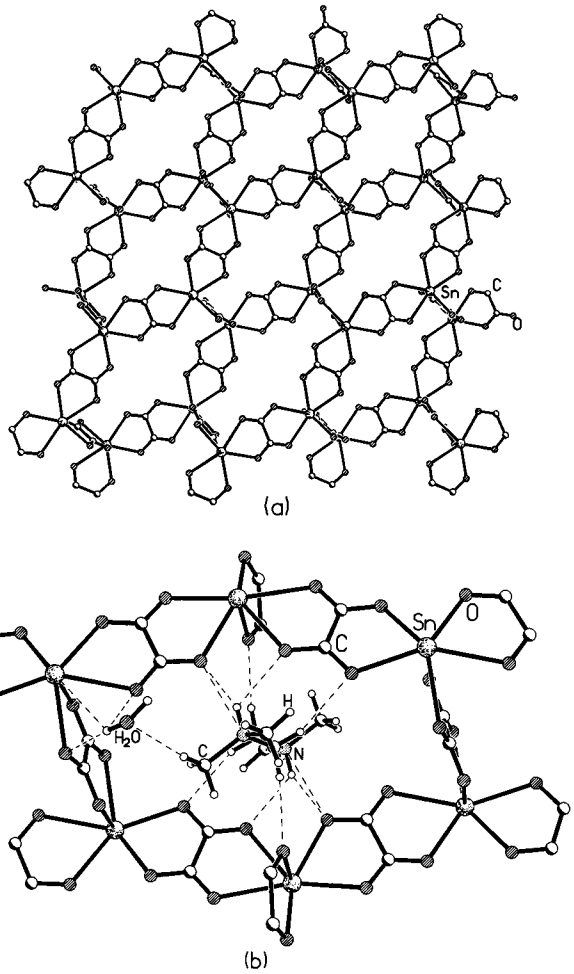

Figure 2. (a) Structure of **I**, $[(CH_3)_2NH(CH_2)_2NH(CH_3)_2]^{2+}[Sn_2(C_2O_4)_3]^{2-}\cdot H_2O$ along the *a* axis showing the 12-membered aperture within one singe layer. (b) Figure showing the hydrogen-bond interaction of the amine and water molecules with the framework within a 12-membered aperture.

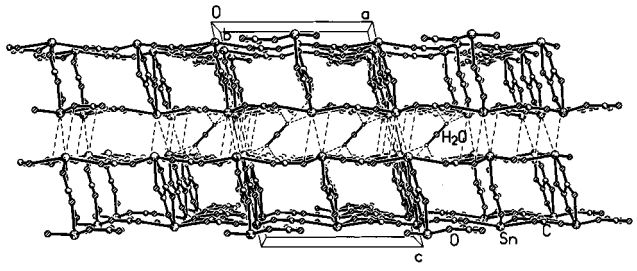

Figure 3. Structure of **I**, $[(CH_3)_2NH(CH_2)_2NH(CH_3)_2]^{2+}[Sn_2(C_2O_4)_3]^{2-}\cdot H_2O$ along the *b* axis showing the 8-membered aperture and the interactions between the water molecules and the framework layers. Note that the dotted lines also show the interactions between the tin atoms (lone-pair interactions) (amine molecules are not shown for clarity).

pentagonal-bipyramidal coordinations are obtained by taking the lone pair of electrons into consideration. The linking of the SnO_4 and SnO_6 units with the C_2O_4 moieties results in an unique saw-tooth layered network, as shown in Figures 6 and 7. These figures also show the various hydrogen-bonding interactions exist between the guest species and the framework tin(II) oxalate. The sheets contain 20-membered corrugated rings (Figure 8) wherein two guanidinium cations and two water molecules reside (Figure 8b). The guanidine molecules are present within the plane of the layer and are held together through hydrogen-bonding interactions with the oxygens of the framework. This is further confirmed by the short O···H distances (1.972−2.277 Å) and the bond angles larger than 150° (the ideal angle for a linear/planar interaction is 180°). Similar interactions involving guanidinium cations have been observed in layered phosphates.[27,28] These structural parameters (Table 8) are in agreement with those reported in the literature for this type of bonding; such interactions are

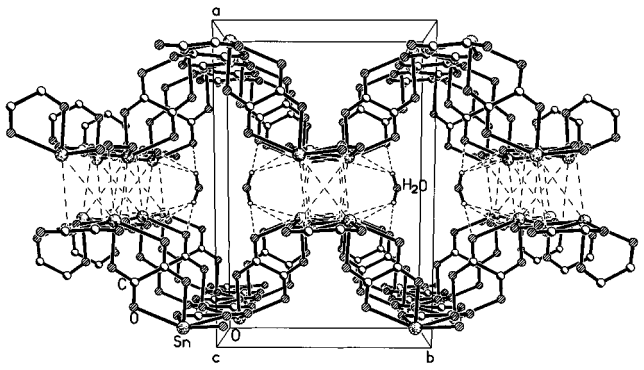

Figure 4. Structure of **I**, $[(CH_3)_2NH(CH_2)_2NH(CH_3)_2]^{2+}[Sn_2(C_2O_4)_3]^{2-}\cdot H_2O$ along the *c* axis showing the layers and the water molecules. Dotted lines represent the various interactions between the layers and the guest species (see text).

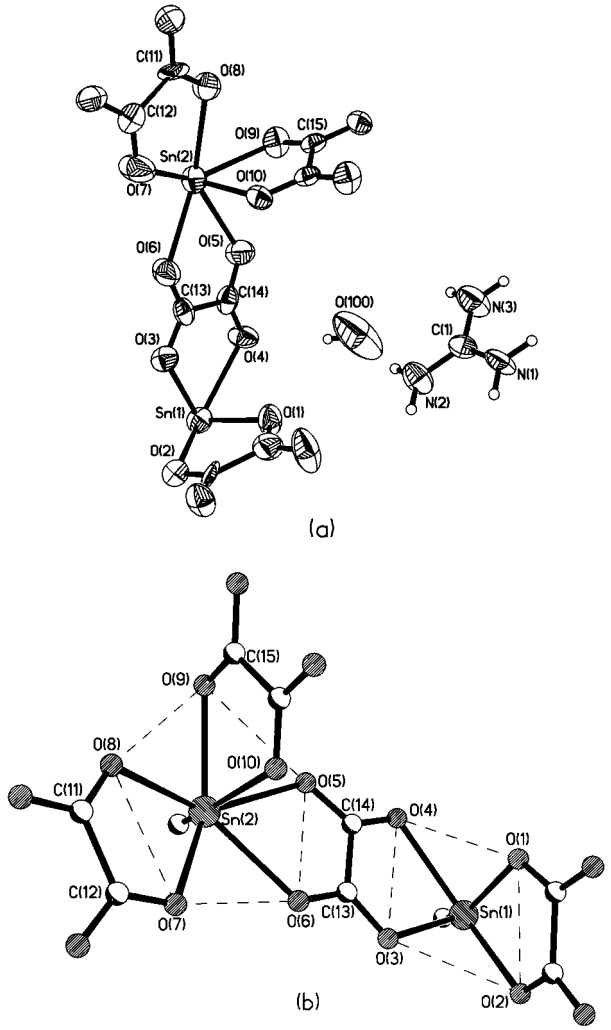

Figure 5. (a) ORTEP plot of **II**, $2[C(NH_2)_3]^+[Sn_4(C_2O_4)_5]^{2-}\cdot 2H_2O$ showing the connectivity (asymmetric unit is labeled). Thermal ellipsoids are given at 50% probability. (b) Figure showing the pentagonal bipyramidal arrangement around one of the Sn atoms and square-pyramidal arrangement around the other Sn (partly filled circle represent the lone pair of electrons).

known to occur in two-dimensional organic porous solids.[16] The presence of the amine molecules within the plane of the pores in **II** also suggests that the large

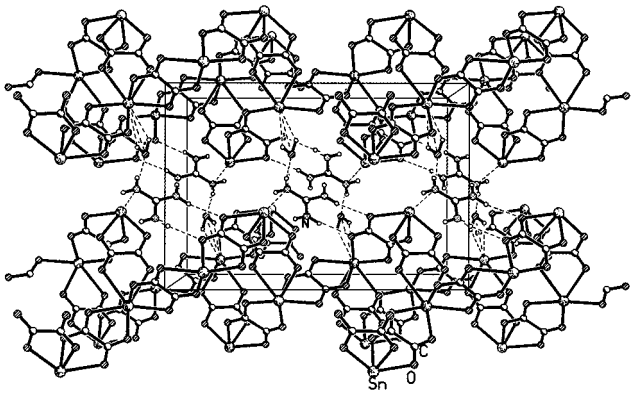

Figure 6. Structure of **II**, $2[C(NH_2)_3]^+[Sn_4(C_2O_4)_5]^{2-}\cdot 2H_2O$ along the *b* axis showing the layer arrangement and the amine and water molecules.

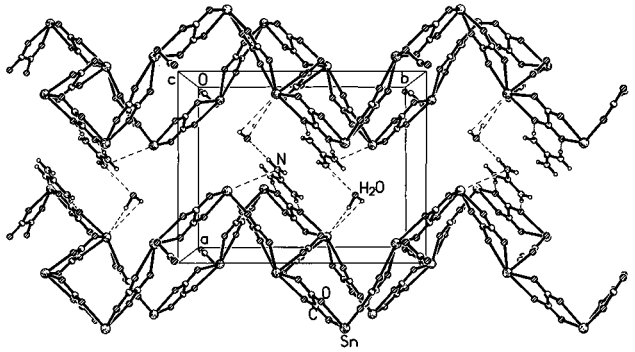

Figure 7. The saw-tooth layered structure of **II**, $2[C(NH_2)_3]^+[Sn_4(C_2O_4)_5]^{2-}\cdot 2H_2O$ along the *c* axis.

apertures are a consequence of the occupation of the guest molecules within the apertures and are necessary to provide the structural stability. Removal of the guest molecules generally leads to the collapse of the framework structure.

The Sn−O bond distances are all in the range 2.197−2.567 Å [$(Sn(1)-O)_{av}$ = 2.287 Å; $(Sn(2)-O)_{av}$ = 2.434 Å] and O−Sn−O bond angles are in the range 64.9−144.7° [$(O-Sn(1)-O)_{av}$ = 86.6°; $(O-Sn(2)-O)_{av}$ = 94.3°] (Tables 6 and 7). The C−O bond distances and angles are also as expected.

TGA of **I** and **II** was carried out in static air from room temperature to 900 °C. For **I**, the weight loss occurs in two steps. A sharp mass loss of about 18% at 300 °C corresponds to the loss of the amine along with the hydrogen-bonded water moleclules (calcd 21.3%) and the loss of about 16% in the region 360−440 °C corresponds to the loss of carbon dioxide from the oxalate group. For the material **II**, the results indicate three steps. A mass loss of 3% occurring below 200 °C corresponds to the loss of water molecules (cald 3.3%), the loss of 11% in the region 220−400 °C corresponds to the loss of the amine molecules (calcd 11.6%), and a sharp loss of 8% around 450 °C might correspond to the loss of carbon dioxide from the oxalate group. The powder XRD patterns of the decomposed products indicated a poorly crystalline nature with very weak reflections corresponding to SnO (JCPDS: 13−111).

Discussion

Two new tin oxalates, $[(CH_3)_2NH(CH_2)_2NH(CH_3)_2]^{2+}[Sn_2(C_2O_4)_3]^{2-}\cdot H_2O$ (**I**) and $2[C(NH_2)_3]^+[Sn_4(C_2O_4)_5]^{2-}\cdot$

(27) Harrison, W. T. A.; Phillips, M. L. F. *Chem. Mater.* **1997**, *9*, 1837.
(28) Harrison, W. T. A.; Bircsak, Z. *Inorg. Chem.* **1998**, *37*, 3204.

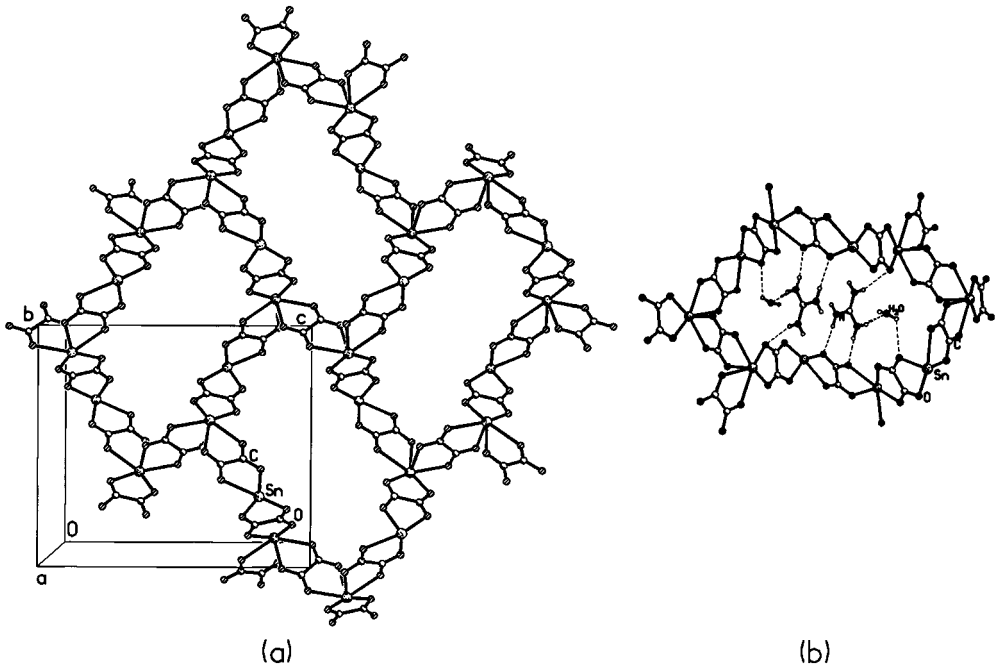

Figure 8. (a) Figure showing the 20-membered apertures arranged in **II**, $2[C(NH_2)_3]^+[Sn_4(C_2O_4)_5]^{2-}\cdot 2H_2O$ along the *a* axis. (b) Figure showing the hydrogen bond interaction of the amine and water molecules with the framework within a 20-membered aperture.

Table 8. Important Hydrogen Bond Distances and Angles in Compounds I and II

moiety	distance (Å)	moiety	angle (deg)
Compound **I**			
O(3)−H(7)	2.143(1)	O(3)−H(7)−N(1)	158.5(1)
O(2)−H(101)	2.380(1)	O(2)−H(101)−O(100)	174.3(1)
O(100)−H(3)[#]	2.395(1)	O(100)−H(3)−C(1)	167.5(1)
O(5)−H(8)	2.497(1)	O(5)−H(8)−C(3)	160.4(1)
O(4)−H(9)	2.434(1)	O(4)−H(9)−C(3)	162.3(1)
Compound **II**			
O(3)−H(1)	2.162(1)	O(3)−H(1)−N(1)	175.2(1)
O(5)−H(2)	2.096(1)	O(5)−H(2)−N(1)	170.5(1)
O(6)−H(3)	2.105(1)	O(6)−H(3)−N(1)	164.7(1)
O(100)−H(4)[a]	1.972(1)	O(100)−H(4)−N(2)	167.7(1)
O(7)−H(5)	2.277(1)	O(7)−H(5)−N(3)	150.7(1)
O(4)−H(6)	2.133(1)	O(4)−H(6)−N(3)	169.2(1)

[a] Intralayer.

$2H_2O$ (**II**), have been synthesized by hydrothermal methods and the structures have been determined. Since the synthesis involves kinetically controlled solvent-mediated reactions, there is no apparent correlation between the starting composition and the stoichiometry of the solid product. The materials **I** and **II** are members of the family of low-dimensional framework solids, essentially possessing two-dimensional, layered architectures. Although, they both involve bonding between the oxalate units and tin atoms, they exhibit distinct differences. The layers in **I** have 8- and 12-membered apertures, whereas **II** has only tortuous 20-membered apertures. While the latter has 6-coordinated Sn(2) atoms and 4-coordinated Sn(1) atoms linked via the oxalate moieties, the former material **I** only has 6-coordinated Sn. The 6-coordinated tin atoms in these oxalates have an unusual coordination, akin to the classic 14-electron systems such as $[IF_6]^-$. This feature is observed in a previous tin(II) oxalate structure as well.[19] The presence of the 4-coordinated Sn atoms seems to be necessary for the formation of large voids by linking with the 6-coordinated Sn atoms via the oxalate moieties. Although large apertures are known to occur within many framework solids, including layered materials,[29] 20-membered rings are rarely observed. Examples of such apertures and channels are very few,[30,31] the apertures being generally restricted to a maximum of 12-membered rings.[32,33] The tin(II) oxalate **II** appears to be the first example of a carboxylate with such large voids. These pores penetrate the entire structure in a direction perpendicular to the sheets, thus yielding a solid with unidimensional channels (∼8.1 × 15.5 Å; longest atom−atom contact distance not including the van der Waals radii) which contain the SDA and water.

The lone pairs of the tin atoms play an important role in the structures of **I** and **II**. The stereoactive lone pairs manifest themselves in the lattice by creating open spaces such as the space between the two layers in these tin oxalates. Similar lone-pair positionings have been observed in many of the layered tin(II) phosphate and related materials.[34,35] The interlayer spacing is shorter in **I** compared to **II** (Figures 3 and 4, and 6 and 7), indicating that other factors are also important as well in directing the formation of these structures.

The coordination environment of Sn(II) atoms in phosphates and oxalates presents an interesting comparison. Most of the tin(II) phosphates have 3- or 4-coordination, forming a trigonal-pyramidal SnO_3 or

(29) Thomas, J. M.; Jones, R. H.; Chen, J.; Xu, R.; Chippindale, A. M.; Natarajan, S.; Cheetham, A. K. *J. Chem. Soc., Chem. Commun.* **1992**, 929.
(30) Estermann, M.; McCusker, L. B.; Baerlocher, Ch.; Merrouche, A.; Kessler, H. *Nature* **1991**, *352*, 320.
(31) Huo, Q.; Xu, R.; Li, S.; Ma, Z.; Thomas, J. M.; Jones, R. H.; Chippindale, A. M. *J. Chem. Soc., Chem. Commun.* **1992**, 875.
(32) Harrison, W. T. A.; Hannooman, L. *Angew. Chem., Int. Ed. Engl.* **1997**, *36*, 640 and references therein.
(33) Chidambaram, D.; Neeraj, S.; Natarajan, S.; Rao, C. N. R. *J. Solid State Chem.* **1999**, in press.
(34) McDonald, R. C.; Eriks, K. *Inorg. Chem.* **1980**, *19*, 1237.
(35) Jordan, T. H.; Schroeder, L. W.; Dickens, B.; Brown, W. E. *Inorg. Chem.* **1976**, *15*, 1810.

distorted square-pyramidal SnO_4 moieties.[20−24] In the oxalates under discussion, we have higher coordination numbers ranging from 4 to 6 (SnO_4 or SnO_6). This is probably because the average charge per oxygen on the oxalate (0.5) is less than that on the phosphate (0.75) and more oxalate oxygens are therefore needed to satisfy the valence of tin.

It is to be noted that both **I** and **II** were synthesized by an adjustment of the pH of the synthetic mixture (different phases are formed at lower pH[22,24]) and the synthesis was effected at near neutral pH. We believe that the phosphoric acid in the initial synthesis mixture essentially acts as a mineralizer, similar to F^- ions in some of the phosphate-based framework solids reported in the literature,[36,37] rather than forming part of the framework (synthesis of phosphate framework materials is generally carried out under acidic conditions). We are presently pursuing this approach further, by exploring the effect of HCl and other additives on the oxalate structures obtained by hydrothermal methods.

On the basis of the structures of **I** and **II** and the hydrogen-bond and lone-pair interactions present in them, a tentative mechanism for the formation of these materials may be proposed. In the case of **II**, the structure-directing guanidinium cation, adopts a side-on approach and forms structurally significant N−H···O bonds (Figure 8 and Table 8). In earlier studies of layered solids, the guanidinium cation directs the formation of essentially 12-membered apertures.[27,28] In **II**, there are two guanidinium cations along with two water molecules in the 20-membered aperture, which interact with the framework through hydrogen bonds. These interactions, along with the position of the amine and water molecules, impose constraints on the framework and give rise to two different coordinations for the tin atoms, leading to the formation of extra-large apertures. Interaction between the protonated amine and water with the framework in **I** leads only to 6-coordinated tin atoms and 12-membered apertures. While the energy changes involved in the interconversions of the rings are likely to be minimal, further work is necessary to understand the mechanism of formation of the variety of open-framework structures in the presence of SDA.

Acknowledgment. The authors thank Unilever plc for providing a research grant in support of our UCSB-JNCASR joint program.

CM990124E

(36) Chippindale, A. M.; Natarajan, S.; Thomas, J. M.; Jones, R. H. *J. Solid State Chem*. **1994**, *111*, 18.
(37) Guth, J. L.; Kessler, H.; Wey, R. *Stud. Surf. Sci. Catal*. **1986**, *28*, 121. Férey, G. *J. Flurorine Chem*. **1995**, *72*, 187.